Review of Some Mathematical Models Used in VisiMix

Simulation of Mixing-Related Processes for Chemical Engineers

Mixing in low viscosity fluids
and multiphase systems

Flow pattern, phase distribution,
heat and mass transfer

VisiMix Ltd., P. O. Box 45170 Har Hotzvim Jerusalem 91450 Israel
Tel. 972-2-5870123 Fax 972-2-5870206 E-mail: info@visimix.com

TABLE OF CONTENTS

SECTION 1. INTRODUCTION **3**
SECTION 2. TANGENTIAL VELOCITY DISTRIBUTION. MIXING POWER. **5**
SECTION 3. AXIAL CIRCULATION **7**
SECTION 4. MACRO-SCALE EDDY DIFFUSIVITY **9**
SECTION 5. MAXIMUM INTENSITY OF MICRO-SCALE TURBULENCE **10**
SECTION 6. SINGLE-PHASE LIQUID MIXING. MIXING TIME **12**
SECTION 7. "NON-PERFECT" SINGLE-PHASE REACTOR **15**
SECTION 8. PICK-UP OF PARTICLES FROM THE TANK'S BOTTOM **16**
SECTION 9. AXIAL DISTRIBUTION OF SUSPENDED PARTICLES **18**
SECTION 10. LIQUID-SOLID MIXING. RADIAL DISTRIBUTION OF SUSPENDED PARTICLES **19**
SECTION 11. LIQUID-LIQUID MIXING. BREAK-UP AND COALESCENCE OF DROPS **20**
SECTION 12. HEAT TRANSFER **23**
SECTION 13. MASS TRANSFER IN LIQUID-SOLID SYSTEMS **26**
SECTION 14. MECHANICAL CALCULATIONS OF SHAFTS **28**
SECTION 15. CONCLUSION **31**
NOTATION **32**
LITERATURE **34**
APPENDIX. MAIN EQUATIONS OF JACKET-SIDE HEAT TRANSFER **36**
NOTATION 37
LITERATURE 37

SECTION 1. INTRODUCTION

The modern approach to the analysis of physico-chemical phenomena and processes, as well as the prediction of their course and results, is based on mathematical modeling. In the past 30 years, the mixing of liquids became a well entrenched subject of research in this direction. A number of sophisticated mathematical models and several highly advanced simulation software packages have been developed. These years were also characterized by rapid progress in the accumulation of new experimental data and the development of new experimental correlations [1-4]. Unfortunately, a wide gap separates these scientific results from routine work of most chemical and process engineers dealing with mixing processes and equipment.

Application of new experimental results and correlations requires, in most cases, an extensive background in the field of mixing. Similarly, the existing CFD (Computational Fluid Dynamics) software for mathematical simulation, such as "Fluent "[5] , can only be used by professionals who have expertise in the field of mathematical modeling. These programs are capable of performing a relatively fast numerical solution of basic equations of flow dynamics. However, in order to obtain a solution for a real problem, the user must actually create a model of the object (tank and process) and formalize it according to the "language" of the software package. This work obviously requires a very high qualification and special training. As a result, this type of software serves as a tool for research work rather than for technical calculations. In addition, its results are purely theoretical, and cannot be relied upon without experimental verification.

The mathematical models and calculation methods used in the VisiMix software have been developed in order to bridge this gap and to make mathematical modeling of mixing phenomena, including average and local characteristics of mixing flow, distribution of concentration and specific features of real “non-perfect” mixing, etc., accessible not only to a researcher, but to every practicing chemical engineer.

Unlike the existing CFD software, or experimental correlations, VisiMix is based on physical and mathematical models of phenomena taking place in mixing tanks. These models are based on all the known data on mixing published in literature. They have been developed as a result of over 30 years’ systematic theoretical and experimental research aimed specifically at developing a method for technical calculations of mixing equipment. The results of this research were published in 2 books [2, 6] and a number of articles during 1960 -1996.

These mathematical models and methods of calculation are based on fundamental equations of turbulent transport of energy, momentum and mass. These equations were formulated and simplified using experimental data on flow pattern and other specifics of agitated flow. Specific conditions, such as boundary conditions on solid surfaces or characteristic scales of turbulent exchange, are described using experimental correlations obtained for a wide range of conditions. The models do not include any mixing parameters that must be estimated experimentally before calculations.

Every model is subject to experimental verification, and most models have been tested on industrial scale and used in engineering practice for many years. These mathematical models and methods of calculations form a single system which allows for performing a chain of consecutive steps of mathematical simulation shown schematically in Fig. 1.

Below is a short review illustrating our approach to the modeling, as well as the theoretical and experimental background of the models used in VisiMix.

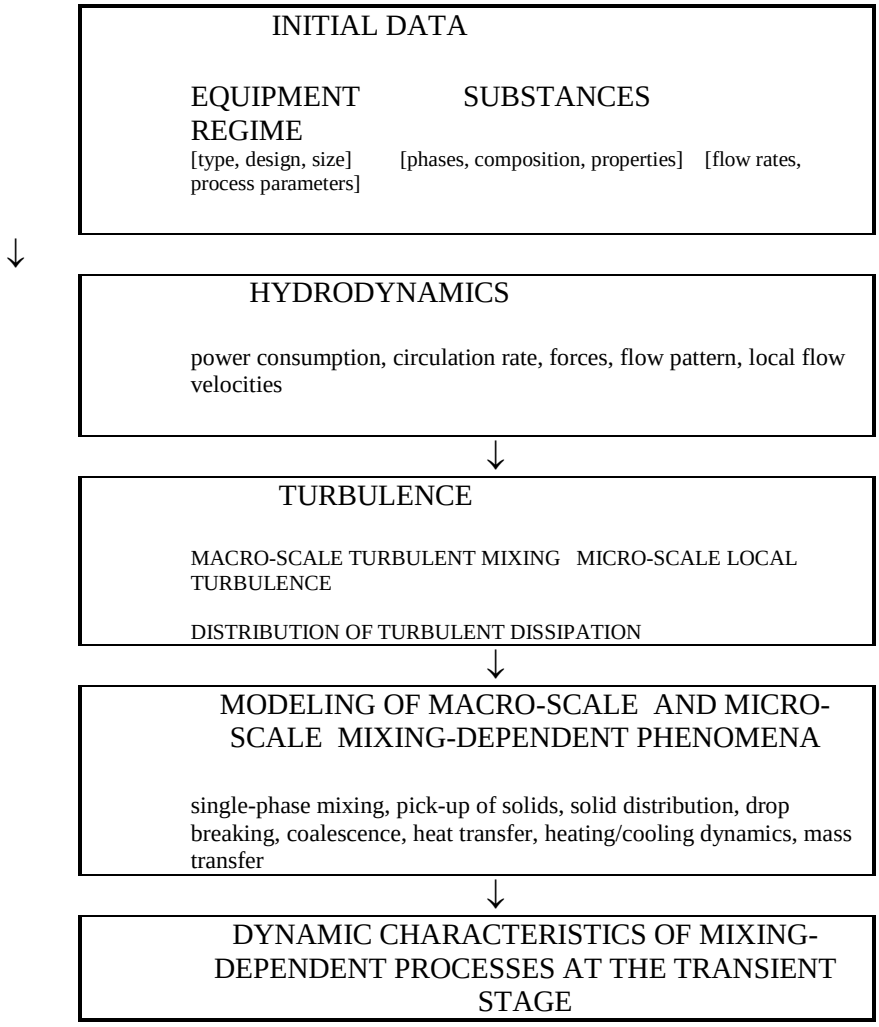

Fig. 1. Flow chart of the mathematical model and calculations (the algorithm).

SECTION 2. TANGENTIAL VELOCITY DISTRIBUTION. MIXING POWER.

The mathematical description of the tangential flow is based [2] on the momentum balance. For steady state conditions, the general equilibrium is presented as the balance of the agitator torque and flow resistance moments of the tank wall, its bottom and baffles; these moments are expressed in terms of flow resistance and calculated using empirical functions for the resistance factors (f_w, f_{bl}, etc., see Fig. 2):

$$M_{agt} = 0.5\, f_{bl}\, N_{agt}\, N_{bl}\, \rho \int_0^{R_{agt}} (\omega r - v_{tg})^2\, H_{bl}\, r\, dr, \qquad (2.1)$$

$$M_{wall} = f_w \rho v_{tg}^2 \pi H R_T^2 \qquad (2.2)$$

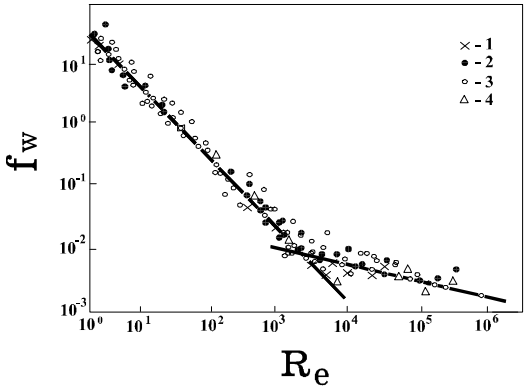

Fig. 2. Wall flow resistance factor, f_w in tanks with different agitators. Tank diameter: 0.3 to 1.0 m; agitators: 1, 2 - turbines; 3 - paddle; 4 - propeller. $R / R_{agt} \geq 2.0$. $Re = W_{av} R_T / \nu$

The system includes also an equation of the turbulent transfer of shear momentum expressed in terms of the "mixing length" hypothesis:

$$dM / dr = 2\pi H\, d(\tau r^2) / dr, \qquad (2.3)$$

$$\tau = \rho L^2 (dv_{tg} / dr + v_{tg} / r) \left| dv_{tg} / dr + v_{tg} / r \right| \qquad (2.4)$$

Values of the resistance factors have been estimated independently using the results of measurements of velocity distribution and torque in 0.02 to 1 cub. m vessels with more than 20 types of agitators of different shape and size. The range of measurements was as follows: Re: up to 2000000, the D_T/D_{agt} ratio: 1.0 ÷ 15, the H/D_T ratio: 0.5 ÷ 3.5, number of agitators on the shaft: 1 ÷ 4. The value of mixing length, L was estimated by comparing the results of the numerical solutions of the equations to the experimental velocity profiles. The agreement between these results and experimental data is illustrated in Fig. 3. For practical purposes, the numerical solution has been replaced with approximate analytical expressions; the parameters of these expressions are calculated using the equations of the momentum balance.

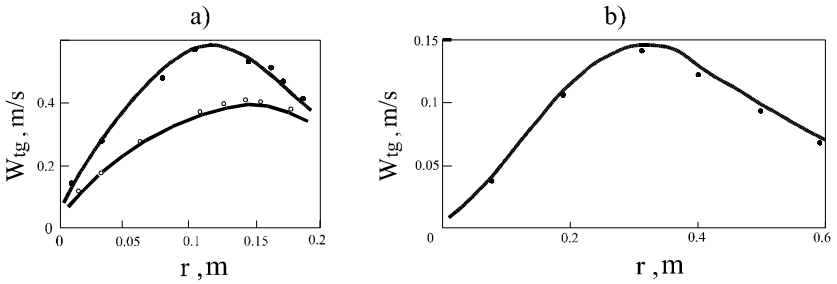

Fig. 3. Experimental and calculated values of the tangential velocity, w_{tg} profiles for a) tank of diameter 0.4 m equipped with the frame agitator, and b) tank of diameter 1.2 m with the twin-blade agitator.

The torque values (Eq. 2.1) are also used for the calculation of mixing power:

$$P = \omega_0 M_{agt} \qquad (2.5)$$

SECTION 3. AXIAL CIRCULATION

The description of the meridional circulation is based [7] on the analysis of energy distribution in the tank volume, and the calculations are performed using the results of modeling of the tangential flow. According to Eq. 2.1, the total power used by the agitator depends on the difference in velocities of the tangential flow and the agitator blades. A part of this energy estimated as

$$P_{bl} = 0.5\, f_{bl}\, N_{bl} \rho \int_0^{R_{agt}} (\omega_0 r - v_{tg})^3\, H_{bl}\, \mathrm{Sin}(\alpha)\, r\, dr \qquad (3.1)$$

is spent on overcoming the flow resistance of the blades; it is transformed into kinetic energy of local eddies and dissipated in the vicinity of the agitator. The other part of the energy is spent in the main flow on overcoming the flow friction. In baffled vessels, i.e. when tangential velocity component is low, the major part of this energy is spent in meridional circulation, mainly for the change of the flow direction and turbulent flow friction [7]:

$$\varphi P = 2\pi H \rho \int_0^{R_T} \nu_E (dv_{ax}/dr)^2\, r\, dr + f_t\, \rho\, v_{ax}^2 / 2q. \qquad (3.2)$$

In this equation, φ is the fraction of the energy dissipated outside the agitator zone:

$$\varphi = (P - P_{bl}) / P \qquad (3.3)$$

These equations are solved in conjunction with the differential equation of local shear stress equilibrium:

$$-\rho \frac{d}{dr}\left(\nu_E r \frac{dv_{ax}}{dr}\right) = 0 \qquad (3.4)$$

The agreement between the calculated and measured values of the circulation number, N_Q is shown in Fig. 4.

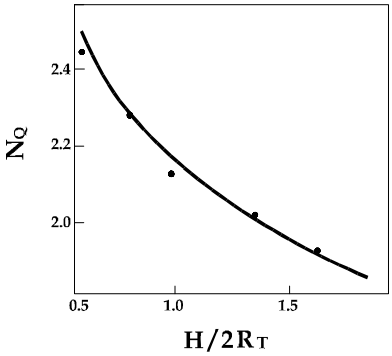

Fig. 4. Experimental and calculated values of the circulation number, $N_0 = q/(n*D^3_{agt})$ as a function of the level of media in the tank. Tank diameter: 0.5 m; agitator: disk turbine.

Axial flow pattern in tanks with multiple agitators is more complicated. As shown experimentally [2] and in [8], the axial circulation in such systems may be described as a superposition of two kinds of axial circulation cycles: local circulation cycles around each agitator, and a general circulation cycle which envelopes the total height of the tank. It has

been found that the values of circulation flow rate for both kinds of cycles depend on the distance between agitators and are directly proportional to circulation flow rate, **q** for a single agitator of the same type and size, calculated as described above (Fig. 5).

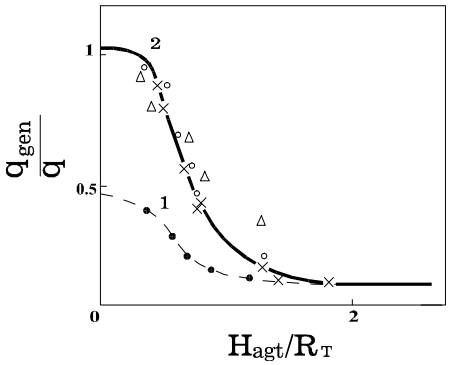

Fig. 5. General circulation in a tank with two-stage agitator.
1 - pitched-paddle agitator; 2 - disk turbine with vertical blades

SECTION 4. MACRO-SCALE EDDY DIFFUSIVITY

From the results of experimental observations and measurements [2], it follows that the modeling of macro-scale transport of mass (solutes and particles) and energy in mixing tanks may be based on a simplified scheme presented in Fig. 6. The parts of the tank volume above and below the agitator are assumed each to consist of two zones differing in the directions of the axial flow. Macro-mixing in each of the zones occurs as a result of simultaneous convection and turbulent (eddy) diffusion, the latter being expressed in terms of the "mixing length" hypothesis:

$$D_{rad} = A_{rad}^2 \, L^2 \, |dv / dr| \quad \text{and} \quad D_{ax} = A_{ax}^2 \, L^2 \, |dv / dr| \qquad (4.1)$$

The exchange between the zones is, furthermore, assumed to be a result of radial velocity in areas of U-turns and radial eddy diffusivity at the boundary radius, r_m. For baffled tanks, the characteristic size is $L \cong R_T$. For unbaffled tanks, $L \cong r_m$ for $r < r_m$ and $L \cong R - r_m$ for $r > r_m$, where radius r_m corresponds to $dv_{tg}/dr = 0$.

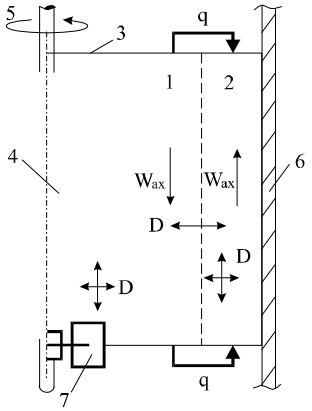

Fig. 6. A simplified scheme of mixing in the turbulent regime. 1 - central zone; 2 - peripheral zone; 3 - upper level of liquid; 4 - shaft; 5 - torque; 6 - wall; 7 - agitator's blade; q - circulation flow rate; D - eddy diffusivity; W_{ax} - average axial circulation velocity

Values of "A" factor in this equation were estimated using the results of measurements of distribution of substances (solutes and particles) and temperature (Fig. 7), and verified by measurements in industrial tanks and basins.

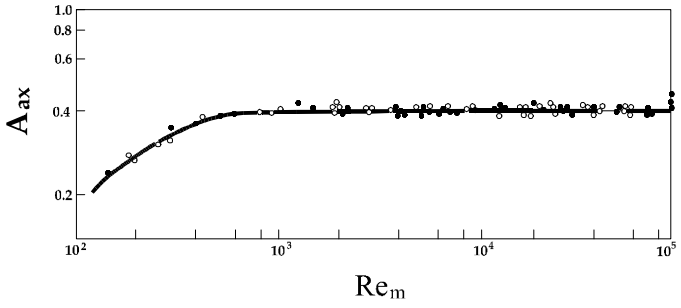

Fig. 7. The mixing length factor, A_{ax} as a function of $Re_m = n * D^2_{agt} / \nu$.

SECTION 5. MAXIMUM INTENSITY OF MICRO-SCALE TURBULENCE

According to the available data, the most intensive turbulence is created in eddies behind the agitator blades, and it is completely dissipated in a turbulent jet formed around the agitator by the discharge flow. In the case of agitators with flat radial blades, the jet is roughly symmetrical with respect to the agitator plane, and its height is about 1.5 of the blade height.

The mathematical description of turbulence distribution in this area required for modeling of micro-scale mixing phenomena such as, for instance, drop breaking, is based on a simplified analysis of transport and dissipation of kinetic energy of turbulence in terms of Kolmogorov's hypothesis of local microscale turbulence.

The mean value of the kinetic energy of turbulence at the radius r is defined as

$$E = 3\bar{v}'^2 / 2,$$

where $\bar{v}'$ is the mean square root velocity of turbulent pulsations corresponding to the largest local linear scale of turbulence, i.e. to the jet height: $l_m \cong h_j \cong 1.5\, H_{bl}$.

Neglecting the influx of turbulence into the jet with axial flow and its generation inside the jet, it is possible to describe steady-state transport of the turbulent component of kinetic energy along the jet radius by equation:

$$q\,(dE / dr) - d\,[2\pi\, r\, h_j\, \nu_E\, (dE / dr)] / dr + 2\pi\, r\, h_j\, \varepsilon = 0, \qquad (5.1)$$

where $\nu_E \cong \bar{v}'\, l_m$. The volume flow rate of liquid, **q** is calculated as shown above.

Eq. 5.1 is solved for $\bar{v}' = 0$ at $r = \infty$. The value of $\bar{v}'$ on the other boundary ($r = R_{agt}$) is calculated using an estimated value of the maximum dissipation rate in the flow past the blades [9, 10]:

$$\varepsilon_m = [\,(\omega_0\, R_{agt} - v_0)\, \mathrm{Sin}\, \alpha]^3 / l_{bl}\,. \qquad (5.2)$$

The dimensions of the ε_m zone (length, height and width) are l_{bl}, H_{bl} and $H_{bl}/2$, respectively. Based on these assumptions, which have been confirmed by experiments [9,11], the mean value of dissipation in the section of the jet at $r = R_{agt}$ is estimated as

$$\varepsilon_0 = \varepsilon_m\, N_{bl}\, H_{bl} / (6\pi\, R_{agt}) \qquad (5.3)$$

Eq. 5.1 is solved numerically. The comparison of calculated results with the data of measurements [13] is shown in Fig. 8.

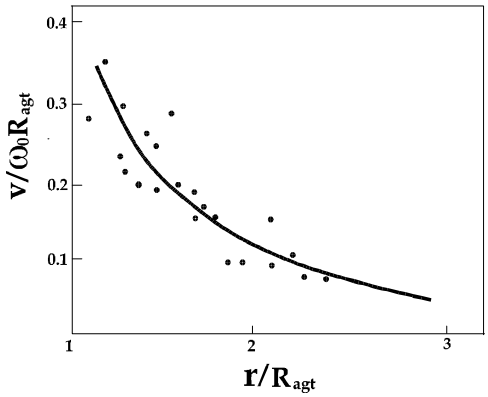

Fig. 8. The RMS velocity fluctuation in the agitator plane as a function of relative radius. The solid line corresponds to the results of the simulation; the data points show published experimental results (disk turbine agitators).

The methods of calculations schematically described above provide the data on the main average and local parameters of flow dynamics as a function of geometry of the agitator/ tank system. These methods create a basis for mathematical modeling of physical and physico-chemical phenomena in application to real processes in mixing equipment. Essential features of some of the models used in VisiMix are described below.

SECTION 6. SINGLE-PHASE LIQUID MIXING. MIXING TIME

Non-steady state space distribution of solute in agitated tanks is described in terms of the model of macro-scale turbulent transport discussed above (Fig. 6).

It was shown by experimental measurements [12] that the reverse "U-turns" of the flow in the upper and lower cross-sections of circulation loops induce equalization of solute concentration even in a laminar flow. The measurements also show [2] that due to this effect and to a relatively high rate of radial eddy diffusivity, it is possible to neglect radial gradient of temperature and concentration inside the upstream and downstream flow zones (obviously, in turbulent regime only), and to describe the solute distribution by equations of a common one-dimensional diffusion model, such as the one presented below for the central zone of the tank (zone 1)

$$\partial C / \partial t = q (\partial C / \partial z) + S_1 D_{1ax} (\partial^2 C / \partial z^2) \qquad (6.1)$$

where $D_{1ax} = 2/ r_m^2 \left(\int_0^{r_m} D_{ax}\, r\, dr\right)$ is the average value of the axial eddy diffusivity in zone 1.

Similar equations are used for the peripheral zone (zone 2, Fig. 6) and for analogous zones below the agitator plane. The system of equations is completed with expressions describing (a) the exchange between the zones resulting from the circulation, eddy diffusivity and mixing in the agitator zone; (b) point of inlet of admixture or tracer and (c) initial conditions corresponding to instant injection of solute (admixture or tracer) into the tank.

The mathematical description of the macroscale transport of substances in tanks with two and more identical agitators placed at a considerable distance from each other (at not less than 0.5 of the agitator diameter) must take into account the following phenomena [2]:

a) Axial circulation of media around each agitator, resulting in the formation of cycles described above;
b) Exchange by eddy diffusivity and circulation inside each of these zones;
c) Exchange between the zones due to the agitators' suction of the media from the two zones, mixing and pumping of the discharge flow into the same zones;
d) Exchange between the zones of two neighboring agitators by eddy diffusivity and circulation.

It should be noted that the boundaries of the zones correspond to maximum values of radial velocity of the media and, accordingly, to a zero value of the velocity gradient. It was shown earlier [2, 14, 15] that such surfaces are characterized by minimum values (and according to Prandtl hypothesis, by zero values) of the eddy diffusivity and by the abrupt change of concentration or temperature in their vicinity. This data allows for concluding that a random eddy-initiated exchange between the zones is much less significant than the mixing around the agitators and the general circulation flow.

Mixing time is estimated as the time required for decreasing the maximum difference of local concentrations in the tank to 1% of the final average tracer concentration. It must be taken into account that the mixing time value represents the characteristic time needed to achieve the uniformity of the solution with respect to the linear macro-scale which is close to the mixing length by order of magnitude (see above). In order to evaluate the time of mixing

required for equalizing the composition in small scale samples, the micro-mixing time value, θ_{mic} must be added to the calculated mixing time, θ_m .

Estimation of the micro-mixing time is based on Kolmogorov's hypothesis of local microscale turbulence. It is assumed that the distribution of the solute is controlled by the turbulent diffusivity in elementary volumes of a linear scale λ only. λ is given by:

$$\lambda> = (\nu^3/\varepsilon)^{1/4} \qquad (6.2)$$

Inside such and smaller elements, the mixing is mainly caused by molecular diffusivity. In a mixing tank, there are two characteristic values of the scale λ_0 :

1. Maximum micro-scale, λ_{bulk} for the bulk of flow estimated according to Eq. 6.2, with the average turbulent dissipation value in the bulk estimated as

$$\varepsilon = \varphi P / (\rho V) \qquad (6.3)$$

The characteristic time of mixing in such elements is estimated as

$$\theta_1 \cong \lambda_{bulk}^2 / D_{mol} \qquad (6.4)$$

2. Minimum micro-scale, λ_m for area with the highest local dissipation, ε_m (see Section 5) with characteristic micro-mixing time

$$\theta_2 \cong \lambda_m^2 / D_{mol} \qquad (6.5)$$

The liquid media in the bulk of flow is "micro-mixed" within the time θ_1 from entering the mixing tank. On the other hand, it is transported with the circulation flow through the agitator zone with a mean period $\theta_c = V/q$. According to the probability theory, nearly all the liquid will pass through the ε_m zone within a period of 3 θ_c , and the time of micromixing for the media cannot exceed

$$\theta_3 = 3V/q + \theta_2 \qquad (6.6)$$

There are, thus, two independent estimates of the micro-mixing time: θ_1 and θ_3. The lower of the two is selected by the program as the Micro-mixing time, θ_{mic} .

The experimental values of the mixing time depend on the ratio of the sensor size, i.e. characteristic linear scale of measurements, to the mixing length. Since the sensor is usually smaller than the mixing length, the experimental mixing time values are higher than the macroscale mixing time, θ_m and than the sum $\theta_m + \theta_{mic}$, which corresponds to the complete micromixing in all points of the volume.
The comparison of the calculated and experimental values of the mixing time [16-18] is shown in Fig. 9, and a curve of "local tracer concentration vs. time" in Fig. 10.

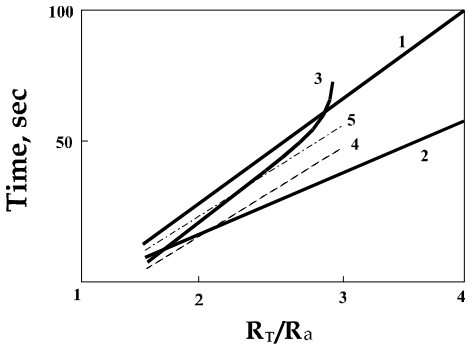

Fig. 9. Mixing time in a tank with a disk turbine agitator as a function of reduced radius.

Simulation results: 1 - micromixing + macromixing, $\theta_{mic} + \theta_m$
2 - macromixing, θ_m
Experimental correlations: 3 - after [16]
4 - after [17]
5 - after [18]

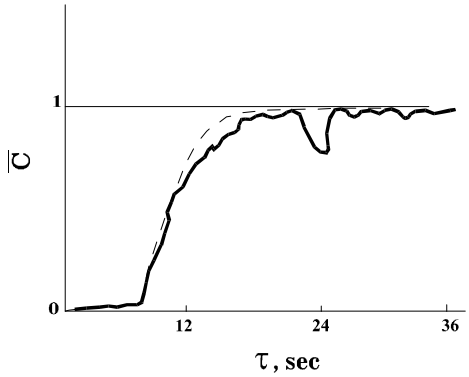

Fig. 10. The change in the tracer concentration in tank with 2-stage pitch paddle agitator (batch blending). Injection point - below the lower agitator, the sensor is located close to the surface of media. The solid line corresponds to the measured data, the dotted line corresponds to the results of simulation.

SECTION 7. "NON-PERFECT" SINGLE-PHASE REACTOR

The simulation of the macro-scale distribution of reactants is also based on the simplified scheme of flow pattern (Fig. 6), and on the main assumptions described above.

Distribution of reactants and its change are described by equations of a common one-dimensional diffusion model, such as the one presented below for reactant "A" distribution along the central zone of the reactor above the agitator:

$$\partial C_a/\partial t = q\,(\partial C_a/\partial z) + S_1 D_1\,(\partial^2 C_a/\partial z^2) - k_r C_a C_b, \qquad (7.1)$$

Analogous equations are used for the reactants "A" and "B" for the second zone above the agitator and for the central and peripheral zones below the agitator. The system is completed with expressions describing (a) the exchange between the zones resulting from the circulation, eddy diffusivity and mixing in the agitator zones; (b) the concentration and flow rate of the inlet flow, and points of inlet and outlet; and (c) initial conditions.

Homogeneous two-component 2nd order chemical reaction
(A + B $\rightarrow$ C) is accompanied by a parallel side reaction and formation of a by-product. Side reactions of two types, i.e.
B + B $\rightarrow$ D and B + C $\rightarrow$ D - are included. Mathematical models used for the simulation are basically similar to the model described in **Single-Phase Liquid Mixing**.

The results of the application of this model to a semi-batch reactor are shown in Fig. 11.

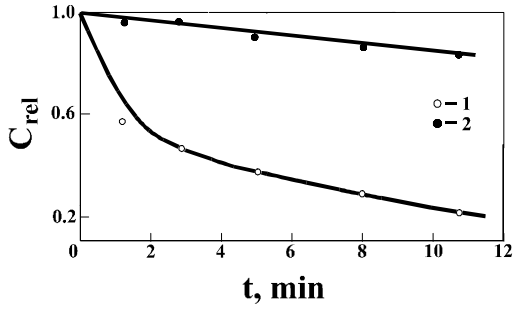

Fig. 11. Time dependence of experimental and calculated values of the local concentration of the reactant "A" in a semi-batch reactor [2]. A fast reaction ($k_r \rightarrow \infty$); $C_{rel} = C_a/C_{a\,0}$. Tank diameter: 0.25 m; radius of agitator: (1) - r = 0.05 m; (2) - r = 0.11 m.

SECTION 8. PICK-UP OF PARTICLES FROM THE TANK'S BOTTOM

The phenomenon of particles pick-up depends on the flow characteristics in liquid layers above the tank bottom. The axial component of the average flow velocity in the vicinity of the bottom is negligible. Therefore the act of picking up a particle from the bottom is regarded as a result of a random fluctuation of pressure, p' above the particle. In a turbulent flow, the fluctuation of pressure is connected to the random instant turbulent fluctuation of velocity:

$$p'_{\lambda} \cong \rho_l \, v'^2/2 \qquad (8.1)$$

The amplitude of the pressure fluctuation, which is capable of picking up the particle must satisfy the following condition:

$$d_p^2 \, p' \geq d_p^3 (\rho_p - \rho_l) g \quad \text{for} \quad \lambda \geq d_p \qquad (8.2)$$

According to Eqs. 8.1 and 8.2, the phenomenon of particle pick-up can be caused by a random pulsation of velocity of a scale $\lambda \geq d_p$, if its amplitude exceeds a "critical" value

$$v_{cr} = \sqrt{2 d_p g \left(\rho_p - \rho_l \right) / \rho_l} \qquad (8.3)$$

The minimum frequency of these pulsations required to prevent accumulation of particles on the bottom is estimated from the condition:

$$dG_{up}/dS \geq dG_{down}/dS \qquad (8.4)$$

where dG_{up}/dS is the flow rate of particles picked up from the bottom calculated as

$$dG_{up}/dS = n \, (v' \geq v_{av}) X_b d_p$$

and dG_{down}/dS is the flow rate of settling particles which is calculated as

$$dG_{down} / dS = W_s \, X_p$$

Therefore, the condition (8.4) assumes the following final form:

$$n_{\lambda} \, \psi(v' \geq v_{cr}) \geq W_s \, X_p/(X_b \, d_p) \qquad (8.5)$$

where $n_{\lambda} = \overline{v'} / \lambda$ is the mean frequency of pulsations of the scale λ, and $\psi(v' \geq v_{cr})$ is the probability of velocity pulsations with amplitude $v' \geq v_{cr}$ expressed using the Gaussian distribution as

$$\psi(v' \geq v_{cr}) \cong 2/\sqrt{\pi} \int_1^{\infty} \exp(-U^2/2) dU,$$

where $U = v' / v_{cr}$

Values of the mean square root pulsation of velocity, v_λ are calculated using common equations of flow resistance and velocity distribution in boundary layer [19]:

$$v_\lambda \cong 1.875\,(\lambda/\delta_o)^{0.33}\sqrt{\tau/\rho}\,; \qquad (8.6)$$

$$\delta_o \cong 11.5\,\nu/\bar{v}_0' \qquad (8.7)$$

Shear stress value, τ is expressed using the experimental correlation for the resistance factor, f_w,, and the values of calculated local velocity of media in those areas of the bottom in which settling is most likely to occur, that is in the central part of the bottom and at the bottom edge ($r = R_T$).

In the case of low concentration, the above system of equations reduces [2] to a simplified equation for the settling radius:

$$r_S \cong 0.19\,R_{agt}\,v_{tg0}\,/\,(W_S\,H^{0.22})$$

The condition for non-settling in the bottom area close to the tank wall is thus $r_S > R$. According to our experimental results, to prevent settling in the central part of the bottom, the minimum value for r_S must be lower than $0.3\,R_{agt}$.

The comparison of the calculated and measured values of the settling radius, r_S is presented in Fig. 12.

VisiMix checks also an additional condition for non-settling: to prevent settling and formation of a static layer of particles, local concentration of suspension near the bottom must be always lower than the concentration of the bulk solid (about 0.6 by volume).

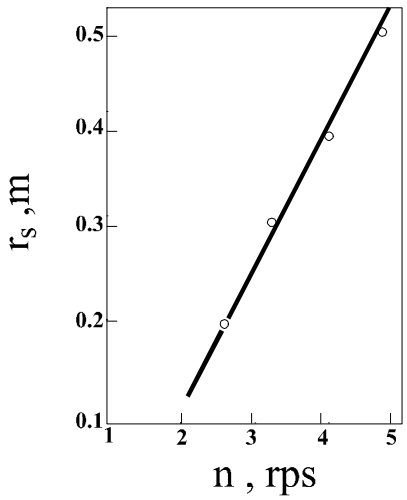

Fig. 12. Radius of settling, r_S as a function of the rotational speed of agitator, n ($D=H$=1m; twin blade agitator of diameter 0.2m ; W_S = 0.018 m/s; $d_p = 10^{-4}$ m). The solid line corresponds to the calculated values.

SECTION 9. AXIAL DISTRIBUTION OF SUSPENDED PARTICLES

The simulation of the axial distribution of solid particles is based on the simplified scheme of flow pattern illustrated in Fig. 6. The transport of particles is assumed to be a result of simultaneous action of average axial flow and macro-scale eddy diffusivity [2, 20]; the spatial distribution of concentration is assumed to correspond to the condition of equilibrium between the transport rate and the rate of separation due to the difference in the densities of phases. For practical cases, it is possible to disregard radial non-uniformity of concentration in each of the zones, and to describe the distribution with equations of the common one-dimensional diffusion model. For the central zone of the tank, axial transport of the solids is described by equation:

$$\partial X / \partial t = (v_{ax} - W_s)(\partial C_a / \partial z) + D_1(\partial^2 X / \partial z^2) \qquad (9.1)$$

An analogous equation is used for the peripheral zones of the reactor. The system is completed with expressions describing:

a) the exchange between the zones resulting from the circulation and eddy diffusivity;
b) conditions and points of inlet and outlet, and
c) initial conditions (see also **Single-phase liquid mixing** above).

The results of the application of this model are shown in Fig. 13.

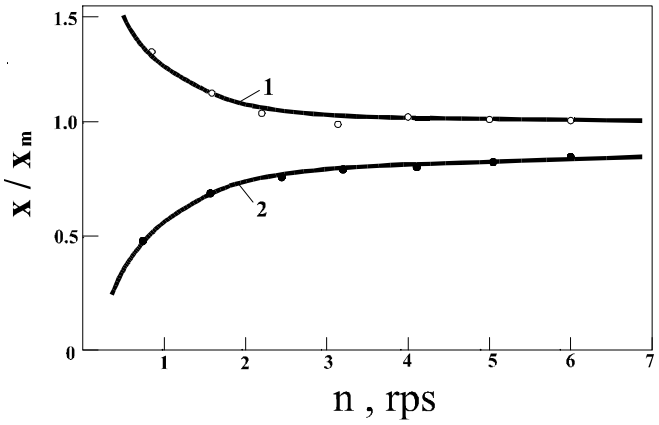

Fig. 13. Concentration of silica gel in kerosene at *h/H*=0.1 (curve 1) and *h/H*=0.9 (curve 2) as a function of the rotational velocity of the agitator (tank diameter is 0.3; impeller, R_T/R_{agt} = 2.15; W_s = 0.00825 m/s). The solid lines correspond to the calculated values.

SECTION 10. LIQUID-SOLID MIXING. RADIAL DISTRIBUTION OF SUSPENDED PARTICLES

The mathematical modeling is based on the description of equilibrium between the centrifugal separation of particles and the radial eddy diffusion with respect to local transport of particles with radial flow in the U-turn zones. For a simplified case of uniform axial distribution, the main differential equation for the central zone (Fig. 6) is:

$$d[2\pi r H (W_{pr} X - D_{rad1} dX/dr)] - 2 q r (X_{av2} - X) dr = 0$$
$$\text{for } r < r_m, \qquad (10.1)$$

where $W_{pr} = W_s (v_{tg} / \sqrt{gr})$ is the settling velocity of particles resulting from the separating effect of the tangential velocity component.

An analogous equation is used for the second zone. The results of the simulation and measurements are shown in Fig. 14.

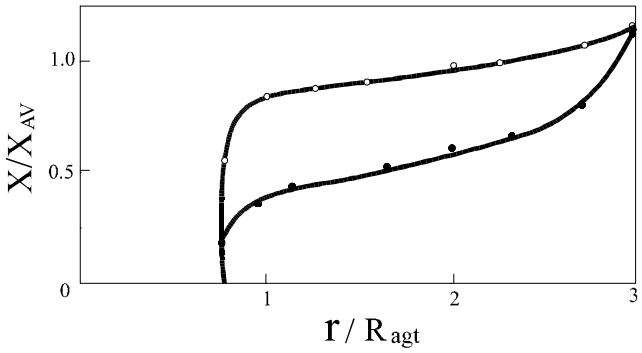

Fig. 14. Experimental and calculated values of the radial distribution of solid phase concentration. Settling velocity of the particles: (1) - 0.01 m/s; (2) - 0.063 m/s.

SECTION 11. LIQUID-LIQUID MIXING. BREAK-UP AND COALESCENCE OF DROPS

The kinetics of the change in the mean drop size in a volume with non-uniform distribution of turbulence is described by equation:

$$dD_m / dt = D_m \int_{(V_T)} (N_c - N_{br})\, dV) / 3Z \qquad (11.1)$$

The break-up of a drop is assumed to occur under the effect of an instantaneous random turbulent velocity pulsation if the amplitude of the pulsation exceeds a certain critical value estimated [11] as

$$v_{cr} \cong 0.775 \left(M + \sqrt{M^2 + 10\sigma / \rho D_m}\right), \qquad (11.2)$$

where $M = \left| 1.2\, \nu_d\, \rho_d / \rho_c - 3\, \nu_c \right| / D_m$.

The mean frequency of the drop break-up in a zone with local turbulent dissipation, ε is given by:

N_{br} = (mean frequency of pulsations of the scale λ_{br}) * (relative frequency of pulsations λ_{br} with amplitude $v' \geq v_{cr}$) * (probability of one or more droplets residing in an area of the scale λ_{br}), i.e.

$$N_{br} = \nu_\lambda\, \psi(v'\, v^*) [1 - \phi(0)]. \qquad (11.3)$$

Here the probability $\psi(v' \geq v^*) \cong \sqrt{2/\pi} \int_1^\infty \exp(-U^2/2) dU$,

where $U = v'/v^*$.

The act of coalescence of droplets is assumed [23] to happen only if two or more droplets are pressed together, for instance, by a turbulent pressure fluctuation, and if the squeezing pulsational pressure is high enough to overcome the repulsive pressure of double layers on the interface. According to DLVO theory [1] [21, 22], the repulsive pressure decreases in the presence of coagulants and increases in the presence of emulsifying agents. Therefore, in order to be "efficient", a random velocity pulsation of the scale $\lambda_c \cong D_m$ must satisfy the following condition:

$$v'_n \geq v^*_c \cong \sqrt{2P_r / \rho_c}\,, \qquad (11.4)$$

where v'_n is the constituent of the pulsational velocity, v' normal to the contact surface of the droplets. According to this model, the mean frequency of coalescence may be defined as

[1] After the names of the authors - Deryagin, Landau, Verwey, Overbeek

N_C = (mean frequency of pulsations of the scale λ_C) ∗ (relative frequency of pulsations λ_c with amplitude $v'_\lambda \geq v^*_C$) ∗ (probability of two or more droplets residing in an area of the scale λ_c), or

$$N_C = n_{\lambda C}\ \psi(v'_\lambda \geq v^*_c)\ (1 - \phi(0) - \phi(1)), \qquad (11.5)$$

where

$$\psi(v'_\lambda \geq v^*_c) \cong [\int_1^\infty (1- V'/V^*)\exp(-V'^2/2)dV']/\sqrt{2P_r/\rho}\ , \qquad (11.6)$$

$\phi(0)$ and $\phi(1)$ are probabilities of zero and one droplet, respectively, residing in the area of the scale λ_c, and

$$V' = v'/v_{\lambda C};\quad V^* = v^*/v_{\lambda C};\quad v_{\lambda C} \cong (\varepsilon\lambda_c)^{0.33}$$

The simulation o the drop break-up/coalescence kinetics is implemented by numerical integration of Eq. 11.1 with respect to the calculated local values of turbulent dissipation in the tank. The results of the simulation for different agitators are shown in Figs. 15 and 16.

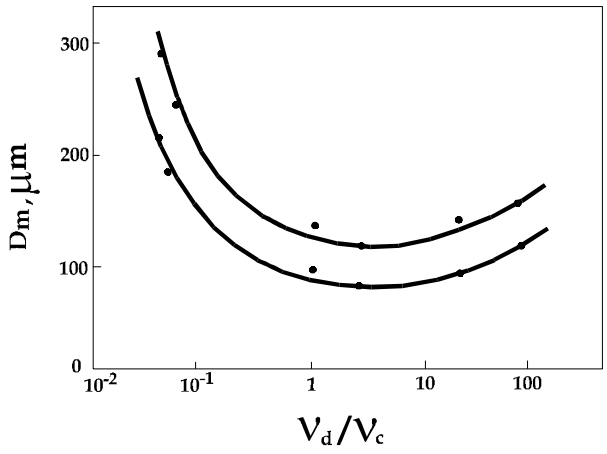

Fig. 15. Mean drop size dependence on the viscosity ratio of phases at two levels of energy input, ε_m:
1: ε_m = 116 W/kg; 2: ε_m = 475 W/kg.
Comparison of experimental and calculated data.

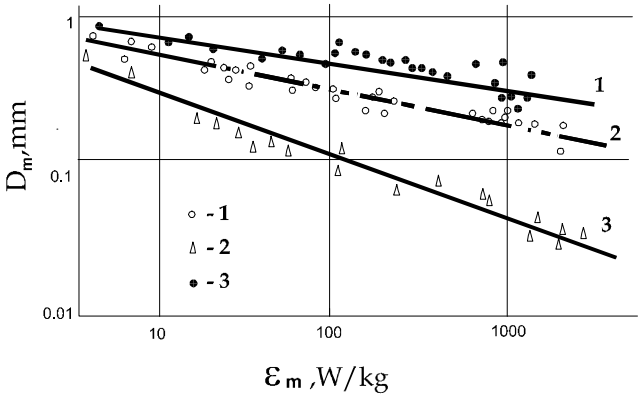

Fig. 16. Drops' break-up and coalescence: Mean drop diameter dependence on the energy input, ε_m. Concentration: 19%. Repulsive pressure: 1 - 7 Pa; 2 - 20 Pa; 3 - ∞.

SECTION 12. HEAT TRANSFER

The mathematical modeling of temperature regimes in mixing tanks with heat transfer devices is based on common equations of heat balance which take into account an eventual change in volume and height of the liquid level in the tank:

$$d(V \rho C_t T)/dt = G_a C_{a,in} T_{a,in} + G_b C_{b,in} T_{b,in} + P +$$

$$+ Q_r + Q_w - (G_a + G_b) C_t T_{out} \qquad (12.1)$$

The change of the active ("wet") heat transfer surface due to vortex formation is also taken into account. In Eq. 12.1, Q_r is expressed with respect to the source of heat release in the reactor. If the heat release is a result of a chemical reaction it is calculated as

$$Q_r = V Ef_r k_r C_a C_b \quad ,$$

$$\text{where} \quad k_r = A \exp - \frac{E_r}{R_g (T + 273)}$$

Heat flux, Q_w from or to the heat transfer device is calculated as

$$Q_w = h S_j (T - T_j), \qquad (12.2)$$

where

$$h = 1/ (1/h_j + R_{tw} + 1/h_m) \qquad (12.3)$$

Values of the jacket-side heat transfer coefficient, h_j are calculated using well known empirical correlations; the equations and sources are presented in the APPENDIX.

The method for calculation of media-side heat transfer coefficients, h_m for mixing tanks with agitators of different types and dimensions is based on the results of the theoretical analysis of eddy conductivity in turbulent boundary layer described in [2, 24]. According to [25], thermal resistance of the turbulent boundary layer on a solid heat transfer surface can be expressed as

$$R_t = \frac{1}{C \rho} \int_0^\infty \frac{dy}{a + a_t} \qquad (12.4)$$

Estimation of the eddy thermal conductivity, a_t in the boundary layer is based [25, 26] on the assumption of its changing as a power function of the distance from the wall. A value of the exponent in this function has been a subject of discussion for some time, and it is estimated by different authors as 4.0 [25] or 3.0 [26]. If we accept the lower estimate,

$$a_t = \bar{v}_0' y^3 / \delta_0^2 \qquad (12.5)$$

we obtain, substituting (12.4) in (12.5):

$$R_t = \frac{1}{C\rho}\int_0^{\infty} \frac{dy}{(\bar{v}'_0 y^3/\delta^2{}_0)+a} \cong \frac{\pi}{2\sqrt{2}}\frac{1}{a\rho C}\sqrt[4]{\frac{a\delta_0^{\,2}}{\bar{v}'_0}}$$

or

$$R_t \cong \frac{0.6\pi}{a\rho C\sqrt{3}}\sqrt[4]{a\delta^2/\bar{v}'_0}$$

and further, using Eqs 6.2 and 8.7,

$$h_m \cong 0.332\rho C(\varepsilon\nu)^{1/4}/\mathrm{Pr}^{2/3}$$

Accepting the higher estimate of the exponent in the expression for a_t, we obtain the following equation:

$$h_m = 0.267\rho C\,(\varepsilon\,\nu)^{1/4}/\mathrm{Pr}^{3/4}$$

The value ε in these equations, which is the value of turbulent dissipation causing the heat transport to the tank surface, is calculated as a function of the power fraction dissipated outside the agitator zone (see Section 4):

$$\varepsilon = P_c/(\rho V)$$

where $P_c = P - P_{bl} = \varphi P$ is the fraction of the power dissipated in the main part of the tank volume calculated using Eq. 3.1.

The comparison of calculated values of Nusselt number, Nu with experimental results obtained by different authors [24-29] has shown that the best agreement between the theoretical results and empirical correlations is achieved if heat transfer coefficient is calculated as the average over the two estimates. Some examples of such comparison are shown in Figs. 17 and 18.

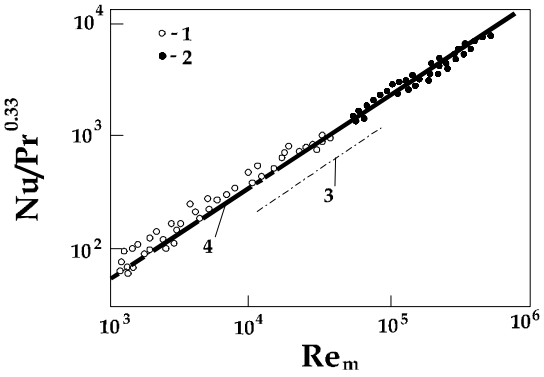

Fig. 17. Heat transfer in tanks with turbine disk agitators. Experimental results after: 1 - [24]; 2 - [25] and 3 - [26]; 4 - the results of calculations.

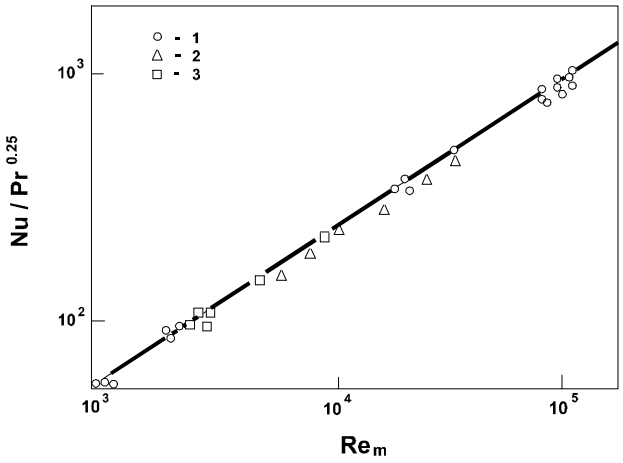

Fig. 18. Heat transfer in tanks with anchor type agitators. Experimental results after: 1 - [27]; 2 - [28]; 3 - [29]; 4 - the results of calculations.

SECTION 13. MASS TRANSFER IN LIQUID-SOLID SYSTEMS

The method for calculating mass transfer coefficients on the surface of suspended particles in a mixing tank is based on Landau's approach to eddy and molecular diffusivity in a turbulent boundary layer [25] in application to mixing [2, 33, 34]. According to [25], a parameter reciprocal to diffusivity that we will call "diffusivity resistance", of the turbulent boundary layer on a solid surface can be expressed as

$$R_D = \int_0^{\infty} \frac{dy}{D + D_{mol}} \tag{13.1}$$

Estimation of the eddy diffusivity, D in the boundary layer is based [25, 26] on the assumption of its changing as a power function of the distance from the wall. The value of the exponent in this function for diffusivity has been estimated by Landau as 4.0 [25].

$$D = \bar{v}_0' y^4 / \delta_0^3 \tag{13.2}$$

By substituting (13.2) in (13.1), we obtain

$$R_D = \int_0^{\infty} \frac{dy}{(\bar{v}'_0 y^4 / \delta^3_0) + D_{mol}} \cong \frac{\pi}{2\sqrt{2}} \sqrt[4]{\frac{\delta_0^3}{D_{mol}^3 \bar{v}'_0}} \tag{13.3}$$

or

$$R_D \cong \frac{0.6\pi}{D_{mol}\sqrt{3}} \sqrt[4]{D_{mol}\delta^2 / \bar{v}'_0} \tag{13.4}$$

and further, using Eqs 6.2 and 8.7,

$$\beta \cong 0.267(\varepsilon\nu)^{1/4} / Sc^{3/4} \tag{13.5}$$

The value ε in these equations is the average value of turbulent dissipation in the tank, and Sc is the Schmidt number equal to ν/D_{mol}.

Comparison of calculated values of mass transfer coefficient with experimental results is presented in Fig.19.

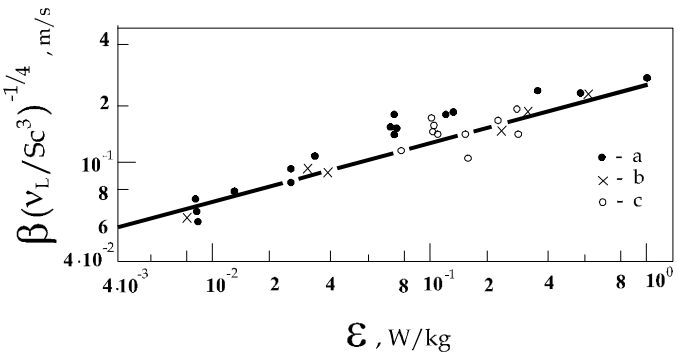

Fig.19. Liquid-solid mass transfer coefficient as a function of energy dissipation in tanks with disk turbine and paddle agitators. The solid line corresponds to calculated results. Experimental data: 1 - [35], 2 - [36], 3 - [33].

SECTION 14. MECHANICAL CALCULATIONS OF SHAFTS

Mechanical calculations are performed in order to check the shaft suitability. The program includes calculations of critical frequency of shaft vibrations and maximum stresses in dangerous cross-sections. The agitator, or all agitators in the case of multistage systems, are assumed to be submerged in the liquid, the central vortex not reaching the agitator. The maximum torque of the agitator drive selected by the user is also used as initial data. Therefore, mechanical calculations are always performed after calculations of hydrodynamics. The program automatically performs a preliminary evaluation, checking the drive selection (power of the drive must be sufficiently high for the selected mixing system) and the vortex depth.

The calculation methods used in the program are related to the vertical console metal shafts with the upper end stiffly fixed in bearings. Three types of shafts are considered:

- A solid stiff shaft with a constant diameter (**regular**);
- A stiff shaft consisting of two solid parts of different diameters (**combined**);
- A stiff shaft consisting of two parts with different diameters - the upper solid stage and the lower hollow (tubular) stage **(combined**).

Both sections of the shaft are assumed to be made of materials with identical mechanical properties. A built-up shaft with stiff couplings is regarded as a single item. The term "stiff shaft" means that the frequency of the shaft rotation (RPM) is less than the shaft's critical (resonance) frequency of vibrations.

Calculations are performed for shafts with one, two or three identical agitators assumed to be fixed on the same shaft stage.

Subject of Calculations and Criteria of Suitability

The program performs three sets of calculations:

1) **Maximum torsional shear stress.** The torque applied to the shaft is assumed to correspond to the maximum value of the driving momentum due to motor acceleration which is 2.5 times higher than the rated torque of the motor. These calculations are performed for the upper cross-sections of the upper and lower stages of the shaft. A single-stage shaft (regular) is regarded as an upper stage of a 2-stage shaft with the length of the lower stage being equal zero. The shaft is considered to be strong enough if the calculated stress value, τ_t is equal to or higher than 0.577 of the yield strength of material:

$$\tau_t = 2.5*M_{dr}*D_s/(2\ I)<0.577\ \sigma_y \qquad (14.1)$$

where I is the 2-nd moment of area, N/m^2;
D_s is shaft diameter, m;
M_{dr} is the drive torque, N*m.

2) **Combined torsion and bending**. The shaft is assumed to be occasionally exposed to a non-even bending force applied to one of the agitator's blades. The maximum combined stress is calculated using the EEUA method [4]. These calculations are performed for the upper cross-sections of the upper and lower stages of the shaft. A single-stage shaft (regular) is considered as an upper stage of a two-stage shaft with the length of the lower stage being equal zero. The shaft is

considered to be strong enough if the calculated stress value is equal to or higher than the yield strength of material:

$$\tau_c + \tau_d < \sigma_y \qquad (14.2)$$

where τ_c is tension created by tcombined bending and torsion moment, and τ_d is direct tension created by the weight of the shaft and agitators.

The bending force is estimated as

$$F_b = Kl*M_{dr}/(4/3R_{agt}) \qquad (14.3)$$

where K1 is the factor of eventual overload, 1.5 - 2.5,

and the corresponding bending moment, M_b is estimated as

$$M_b=F_b*L_{agt;} \qquad (14.4)$$

where L_{agt} is the distance from the calculated cross-section to the lowest agitator.

The stress created by the combined moment is calculated using the formulae :

$$M_b1 = \sqrt{(M_b\ 2 + (K1*M_{dr})2)}\ ;$$
$$M_b2 = (M_b + \sqrt{(M_b 2\ +\ (K1*M_{dr})2)}\ /2; \qquad (14.5)$$
$$M_c = (M_b1 + M_b2)/2;$$

and $\tau_c = M_c*D_s/(2I).$ (14.6)

The direct stress applied to the shaft is

$$\tau_d = 9.81(Z_{agt}*m_{agt} + m)/S, \qquad (14.7)$$

where m_{agt} and m are masses of the agitator and the shaft respectively, and S is the area of the shaft cross-section.

3) **Critical frequency of vibrations.** The shaft is considered to be stiff if the rotational frequency is less than 70% of the calculated critical (resonance) velocity.

The critical frequency is calculated using the formulae:

$$f_{cr} = \omega*\ D_s1/(4L_s)*\sqrt{E/\rho_s} \qquad (14.8)$$

and

$$\omega = \sqrt{K_{st}\ /(\tilde{m}_s + \tilde{m}_a)} \qquad (14.9)$$

where D_s1 is the diameter of the upper stage of the shaft,
L_s is the shaft length,
E is Young's modulus,
ρ_s is the density of the shaft material,
$\tilde{m}_s$ and $\tilde{m}_a$ are the equivalent masses of shaft and agitator, respectively.

Calculation of dimensionless stiffness, K_{st} is based on 2nd moments and lengths of both shaft stages. The equivalent masses of shaft and agitators are calculated using estimated deflection of both stages.

The calculation is based on the method developed by Milchenko et. al. [37, 38] and verified by 20 years of practical application.

SECTION 15. CONCLUSION

The examples presented above illustrate the approach to the problem of modeling and technical calculations in the field of mixing developed and used by the authors of VisiMix and their coworkers in 1960-1996.

The essential features of this approach can be described as follows:

1. **Mathematical models are developed for engineering calculations and for the solution of technical problems of design and application of mixing equipment.**

2. **The main purpose of the modeling is to provide engineers with predictions of parameters of a direct practical interest, i.e. the values of concentrations and temperatures, shear rates, drop sizes, heat- and mass-transfer rates, as functions of mixing conditions, including equipment geometry and dimensions, the properties of the media and the process features.**

3. **The mathematical modeling of mixing phenomena and mixing-dependent unit operations is based on a limited number of key intermediate flow parameters (average velocity distribution, macroscale eddy diffusivities, etc.) and characteristics of turbulence in different parts of the volume. All experimental constants or functions necessary for calculating these parameters have been estimated at the stage of research and development of the models, and engineers do not need any additional information on mixing for applying the models.**

4. **Every mathematical model is a simplified reflection of a real phenomenon; all models are verified by experimental results, including available published experimental data of different authors. The methods for calculating the key flow parameters and most mathematical models were confirmed also by the results of measurements and testing in industrial-scale equipment, and have been used in engineering practice since the end of the 70-s.**

5. **The modeling usually includes several consecutive steps of calculations; therefore, to make the method practical, the software development always includes the analysis and simplification of the main equations with respect to the practical application range in order to reduce the simulation time without impairing the reliability of the obtained results.**

The examples presented above are related to the problems, which are covered by the current version of VisiMix. However, the same approach has been used for investigation and modeling of some other mixing phenomena, such as mixing of high viscosity media (laminar regime) [39], mixing in gas-liquid systems [40], homogenizing multi-component mixtures, etc., and the appropriate sections are planned to be included in future releases of VisiMix. “Laminar flow” module has already been released and incorporated in the new VisiMix product, VisiMix LAMINAR.

NOTATION

C	specific heat capacity, J/(kg.K);
d_p	diameter of particles, m;
D_{mol}	molecular diffusivity, m^2/s;
D	eddy diffusivity, m^2/s;
D_m	mean drop size, m;
E_r	energy of activation, J/Mol,
Ef_r	heat effect of reaction, J/kMol
f_m, f_{bl}	hydraulic resistance factors for wall and blade;
h_m	heat transfer coefficient, media-side
H	level of media in the tank, m
H_{bl}	height of agitator blade, m;
G	mass flow rate, kg/s,
k_r	specific reaction rate;
L	mixing length, m;
l_{bl}	length of blade, m;
M	momentum, J;
N	specific frequency, 1/(cub. m ∗s);
N_{bl}	number of blades;
N_{agt}	number of agitators on the shaft
n_λ	mean frequency of pulsations of the scale λ, 1/s;
P	power, W;
P_r	repulsive pressure, Pa;
Q_w	heat flux from the heat transfer device, W,
Q_r	heat release rate, W,
q	circulation flow rate through agitator, m3/s,
q	rate of general circulation in tanks with multi-stage agitators, m3/s,
R_g	gas constant, J/(mol∗K) ;
R_T, R_{agt}	radius of tank and agitator, m;
S	cross-section of axial flow, m^2;
Sc	Schmidt number
t	time, s;
T	temperature, °C,
v_{tg}	tangential velocity, m/s;
v_{ax}	axial velocity, m/s;
v'	random turbulent constituent of velocity, m/s,
$\overline{v'}$	mean square root velocity of turbulent pulsations, m/s;
V_T	volume of media, m^3;
W_s	settling velocity of particles, m/s;
X_b	concentration of the solid near the bottom, kg/cub. m;
X_p	concentration of the solid kg/cub. m;
α	pitch angle of blades, degrees;
δ_0	thickness of the laminar sublayer, m;
ε	turbulent dissipation rate, W/kg;
λ	linear scale of turbulence, m;
ν	kinematic viscosity, m^2/s;

ν_E	eddy viscosity, m^2/s;
ξ	resistance factor for U-turns of flow;
θ_{mic}	micro-mixing time, s;
τ	shear stress, Pa;
ω_0	angular velocity of agitator, rad/s.

Subscripts: agt - agitator, av - average, ax - axial, bl - blade, br - breaking, c - coalescence, rad - radial, 1 - central zone, 2 - peripheral zone; a, b - reactants A and B, in - inlet flow, out - outlet flow.

LITERATURE

1. Oldshue, J. Y., Fluid Mixing Technology, McGraw-Hill, New York (1983).
2. Braginsky, L. N., Begatchev, V. I. and Barabash, V.M., Mixing of Liquids. Physical Foundations and Methods of Calculations, Khimya Publishers, Leningrad (1984), in translation & update.
3. Tatterson, G. B., Fluid Mixing and Gas Dispersion in Agitated Tanks, McGraw-Hill, New York (1991).
4. Harnby, N., Edwards, M. F. and Nienow, A. W., Mixing In The Process Industry, Butterworth-Heinemann, London (1992).
5. Baker, A. and Gates, L. E., CEP, 1995, 12, 25-34.
6. Modeling of Aeration Basins for Waste Water Purification, Braginsky, L. N., Evilevich, M. A., Begatchev, V. I. et al, Khimya Publishers, Leningrad (1984).
7. Yaroshenko, V. V., Braginsky, L. N. and Barabash, V.M., *Theor. Found. of Chem. Eng.* (USSR), 22, 6 (1988, USA translation-1989).
8. Fort I., J. Hajek and V. Machon, Collect. Czech. Chem. Commun., 1989, v.34, pp 2345-2353.
9. Braginsky, L. N. and Belevizkaya, M. A. *Theor. Found. of Chem. Eng.* (USSR), 24, 4 (1990, USA translation - 1991).
10. Braginsky, L. N. and Kokotov, Y. V., *J . Disp. Sci. Tech.*, 14, 3 (1993).
11. Braginsky, L. N. and Belevizkaya, M. A., *Theor. Found. of Chem. Eng.* (USSR), 25, 6 (1991, USA translation - 1992).
12. Begatchev, V. I. and Braginsky, L. N., "Mixing in Turning Areas of Laminar Agitated Flow", 5th All-Union Conference on Mixing, Leningrad, Zelenogorsk, USSR (19).
13. Costes J., J.F. Couderc, Chem. Eng. Sci., 1987, v.42, N2, p.35-42.
14. Braginsky L.N., V.I.Begatchev and O.N.Mankovsky, Theor.Found.Chem.Engng, 1974, v.8, No.4, pp. 590-596.
15. Braginsky L.N., V.I.Begatchev and G.Z.Kofman, Theor.Found.Chem.Engng, 1968, v.2, No.1, pp. 128-131.
16. Hiraoka S. and R. Ito, J. Chem. Eng. Japan, 1977, v.10, N1, p.75.
17. Shiue, S. J. and C.W. Wong, Canad. J. Chem. Eng., 1984, v.62, p.602.
18. Sano, Y. and H. Usui, J. Chem. Eng. Japan, 1985, 18, N1, p.47.
19. Reynolds A.J. Turbulent Flows in Engineering, Wiley & Sons, New York, 1974.
20. Soo, S. The Hydrodynamics of Multiphase Systems (Transl.),Mir Publishers, Moscow, 1971.
21. Verwey, E.J.W. and Overbeek, J.Th.G., Theory of the Stability of Lyophobic Colloids, Elsevier, Amsterdam (1948).
22. Adamson, A.W., Physical Chemistry of Surfaces, Wiley & Sons, New York, 1976.
23. Braginsky, L. N. and Kokotov, Y. V., "Kinetics of Break-Up and Coalescence of Drops in Mixing Vessels," presented at the 11th International Congress on Chemical Engineering "CHISA", Prague, Czech Republic (1993).
24. Barabash, V.M. and Braginsky, L. N., Eng. - Phys. Journal (USSR), 1981, v. 40, No.1, pp. 16-20.
25. Landau, L.D. and Lifshitz, E. M., Mechanics of Continuous Media, Gostechizdat Publishers, Moscow, 1953.
26. Levich, V.G., Physico-Chemical Hydrodynamics, Physmatgiz Publishers, Moscow, 1959.
27. Chapman, F., Dallenbac, H. and Holland, F., Trans. Inst. Chem. Eng., 1964, v. 42, pp. 398-403.
28. Strek, F., Chemia Stosowana , 1962, No.3, p.329.
29. Strek, F., Karcz, J. and Bujalki, W., Chem. Eng. Technol., 1990, v. 13, pp. 384-392.
30. Uhl, V.W. and Vosnick, H.P. , CEP, 1960, v.56, No.3, p.72.
31. Brown R.W., Scott, R. and Toyne, C. , Trans. Inst. Chem. Eng., 1947, v. 25, p.181.

32. Uhl, V.W., CEP, Symp. Series, 1955, v.51, p.93.
33. Nikolaishvily, E. K., V.M.Barabash, L. N. Braginsky et al, *Theor. Found. of Chem. Eng.* (USSR), 1980, v.14, No.3, pp. 349-357 (USA translation - 1981).
34. Kulov N.N., E. K. Nikolaishvily, L. N. Braginsky and al., Chem. Eng. Commun., 1983, v.21, pp. 259-271.
35. Hixon, A.W. and S.J. Baum, Ind. Eng. Chem., 1942, v. 34, No. 1, p. 120.
36. Barker, J. J. and R.E.Treybal, A.I.Ch.E. Journal, 1960, v. 6, No. 2, p. 289.
37. N. I. Taganov, V. M. Kirillov and M. F. Michalev, Chemical and Oil Machinery (USSR), 1965, No. 10, pp. 11- 14.
38. Milchenko, A. I. et al., Proceedings of the Leningrad R&D Institute of Chemical Machinery (LenNIICHIMMASH), St. Petersburg, 1967, issue 2, pp.78-90.
39. Begachev, V.I., A. R. Gurvich and L. N. Braginsky, *Theor. Found. of Chem. Eng.* (USSR), 1980, v.14, No.1, pp. 106-112 (USA translation - 1980).
40. Barabash, V.M., L. N. Braginsky and G. B. Gorbacheva, *Theor. Found. of Chem. Eng.* (USSR), 1987, v. 21, No. 5 pp. 654-660 (USA translation - 1988).

APPENDIX. MAIN EQUATIONS OF JACKET-SIDE HEAT TRANSFER

Device	Process	Equations	Range	Source
Half-coil	Forced convection	$\mathbf{Nu} = 0.027\ \mathbf{Re}^{0.8}\ \mathbf{Pr}^{0.33} * * (\mu/\mu_w)^{0.14}\ E_t$	Turbulent flow $\mathbf{Re} > 2000$	1
		$\mathbf{Nu} = 3.2\ (\mu/\mu_w)^{0.14}$ $E_t = 1 + 3.6\ D_{hc}/D_T$ $\mathbf{Re} = \rho V_j\ D_{hd}/\mu$ $\mathbf{Pr} = C_t\ \mu / k$ $\mathbf{Nu} = h_j\ D_T / k$ $D_{hd} = 0.61\ D_{hc}$	Laminar flow	2
Half-coil	Condensing steam or vapor	$\mathbf{Nu} = 0.0133\ \mathbf{Pr}^{0.4}\ \mathbf{Re_f}^{0.8} * * (\mu/\mu_W)^{0.25} * X_1$ $X_1 = \sqrt{\rho_j / \rho_v} + 1$ $\mathbf{Re_f} = G_v/(D_{hd}\ \mu)$ $h_j = 0.02\ k \sqrt{(Re_f / 1.67)} * * (L_{hc}/D_{hd})^{-0.2}\ (\mu\ k/(g C_t\ \rho^2))^{-1/3}$	Turbulent flow $\mathbf{Re_f} > 10000$ $\mathbf{Re} \in (15, 2800)$	2, 3 3
Jacket	Forced convection	$\mathbf{Nu} = 1.85(\mathbf{Re\ Pr}\ D_{hd}/H_j)^{1/3}$ $\mathbf{Nu} = 3.72$ $D_{hd} = 2\ W_j$	$\mathbf{Re\ Pr}\ D_{hd}/Hj \geq 70$ $\mathbf{Re\ Pr}\ D_{hd}/H_j < 70$	1
	Free convection	$\mathbf{Nu} = 0.13(\mathbf{GrPr})^{0.3} * (\mu/\mu_W)^{0.25}$ $\mathbf{Nu} = 0.56\ (\mathbf{GrPr}\ \mu/\mu_W)^{0.25}$ $L_C = 9.81\ \beta_t\ \rho\ C_t / \mu\ k$ $\mathbf{GrPr} = H_j^3\ \lvert T_W - T_{j.out} \rvert\ L_C$	Turbulent flow $\mathbf{GrPr} > 10^9$ Laminar flow $\mathbf{GrPr} < 10^9$	4, 8
	Condensing steam or vapor	$h_j = X_1\ \mathbf{Re_f}/(2300+X_2)$ $X_1 = k/(\nu^2/g(1-\rho_V/\rho))^{0.33}$ $X_2 = 41(\mathbf{Re_f}^{0.75} - 89) * * (\mu/\mu_W)^{0.25}/\sqrt{Pr}$	Turbulent flow	4, 6, 9

Device	Process	Equations	Range	Source
		$h_j = 0.943(k^3\ \rho\ (\rho - \rho_V) * * g\ Q_{cond} / (\mu\ (T_{sat} - T_{wj}) * * H_j))^{0.25}\ E_1\ E_2$ $E_1 = (1 + 0.4(T_{sat} - T_{wj}) * * C_t / Q_{cond})^{1/2}$ $E_2 = \mathbf{Re_f}^{0.04}$ $\mathbf{Re_f} = G_v/(\pi D_T \mu)$	Laminar flow	3, 4, 6 3, 7 3

NOTATION

Gr	jacket-side Grashof number;
Nu	jacket-side Nusselt number;
Pr	jacket-side Prandtl number;
Re	jacket-side Reynolds number;
$\mathbf{Re_f}$	Reynolds number for liquid film;
C_t	heat capacity of liquid heating/cooling agent at temperature T_j, Pa∗s,
D_{hc}	diameter of half-coil, m;
D_{hd}	hydraulic diameter of half-coil, m;
D_T	tank diameter, m
G_v	mass flow rate of steam (vapor), kg/s;
h_j	jacket-side heat transfer coefficient, W/(sq. m ∗ K);
k	conductivity of liquid heating/cooling agent at temperature T_j, W/(m ∗K),
Q_{cond}	specific heat of evaporation of heating/cooling agent , J/kg;
T_j	temperature of heating/cooling agent in jacket, C;
T_{sat}	temperature of saturation of steam (vapor), C;
T_{wj}	jacket-side wall temperature, K;
V_j	velocity of heating/cooling agent , m/s;
W_j	width of the jacket channel, m;
E_t	adjusting factors for coils
β_t	specific volume expansion of liquid heating/cooling agent at the temperature T_j, 1/cub. m ∗ K;
μ	dynamic viscosity of liquid heating/cooling agent at the temperature T_j, Pa ∗s,
μ_w	dynamic viscosity of liquid heating/cooling agent at the temperature T_{wj},
ρ	density of liquid heating/cooling agent at temperature T_j, kg/cub. m
ρ_v	density of steam (vapor) in the jacket, kg/cub. m

LITERATURE

1. Wong, H.Y., Heat Transfer for Engineers, Longman, London and New York, 1977.
2. Kutateladze, S. S. Heat Transfer and Hydrodynamic Resistance, Energoatomizdat, Moscow, 1990.
3. Mankovsky, O. N., A. R. Tolchinsky and M. V. Alexandrov, Heat Transfer Equipment of Chemical Industry. Khimya, Leningrad, 1976.
4. Boyko L.D. and G. N. Kruzilin, Izvestia AN USSR: Energetika i Transport, 1966, No.5, pp. 113-128
5. Volkov D.I. Proc. of CKTI, Leningrad, !970, No. 101, pp. 295-305.
6. Incropera, F. P., De Wit, D. P., Fundamentals of Heat and Mass Transfer, Wiley, 1990.
7. Bromley, L. A., Ind. & Eng. Chem., 1952, v. 44, pp. 2966-2996.
8. The Essentials of Heat Transfer II, Research and Educational Association, New Jersey, 1987.
9. Labuntsov. D. A., Heat Transfer in Film Condensation of Pure Steam on Vertical Surface and Horizontal Tubes, Teploenergetika, 4, No. 72, 1957.